

## Compton polarimetry at parity violation experiments

Y. IMAI

*Institut für Kernphysik, Johannes Gutenberg-Universität Mainz - D-55099 Mainz, Germany*

ricevuto il 3 Novembre 2011; approvato il 5 Maggio 2012  
pubblicato online il 3 Luglio 2012

**Summary.** — Beam polarimetry is a vital aspect of accelerator-based parity violation (PV) experiments. So far, Compton backscattering polarimetry is the only method capable of measuring at the nominal beam conditions of the experiment. However, due to the low luminosity achievable with commercial lasers, it is slow compared to other methods using solid-state targets. This article reviews the principles of Compton polarimetry, gives an overview of the methods employed to overcome this disadvantage, and presents recent developments aimed at reaching the demanding precision goals ( $< 1\%$ ) of the next generation of PV experiments.

PACS 29.27.Hj – Polarized beams.

PACS 29.27.Fh – Beam characteristics.

PACS 42.60.Da – Resonators, cavities, amplifiers, arrays, and rings.

### 1. – Introduction

Accelerator-based parity violation (PV) experiments use (longitudinally) polarized beams of alternating helicity to measure count-rate asymmetries in electron scattering. The relevant information, however, is contained in the underlying cross-section asymmetries, which are related to the count-rate asymmetries via the beam polarization  $P_e$ :

$$(1) \quad A_{rate} = P_e A_{c.s.}$$

It is therefore indispensable to perform an absolute beam polarization measurement. The importance of this aspect is further underlined by the fact that the polarimetry error is still the largest contribution to the systematic error budget (see table I).

In order to minimize systematic uncertainties, the polarization measurement must be performed immediately in front of and at the same beam conditions as the PV experiment. Currently, this is only possible using Compton backscattering polarimetry, as the other common methods, Mott and Møller polarimetry, are destructive due to the use of solid-state targets and are limited in the acceptable beam energy (Mott) or current (Møller —work is in progress, however, to overcome this limitation, see *e.g.* [4]).

TABLE I. – *Statistical and systematic errors of recent PV experiments [1-3].*

Experiment	Statistical error	Total systematic error	Polarimetry error
A4 (2008)	4.8%	5.2%	4.0%
HAPPEX-III	3.3%	1.5%	0.9%
G0 ( $H_2$ , high $Q^2$ )	5.2%	1.7%	1.0%

## 2. – Compton backscattering polarimetry

**2.1. Principles.** – Compton polarimetry uses the spin dependence of the electron-photon scattering cross-section by colliding polarized (usually optical) photons with the electron beam and detecting the final-state photon and/or electron. In the case of a polarization-insensitive detector, the photon scattering cross-section is given by [5]:

$$(2) \quad \frac{d\sigma(\vartheta, \varphi)}{d\Omega} = \frac{d\sigma_0(\vartheta)}{d\Omega} + Q \frac{d\sigma_1(\vartheta)}{d\Omega} - VP_e^{long} \frac{d\sigma_2^{long}(\vartheta)}{d\Omega} - VP_e^{trans} \cos \varphi \frac{d\sigma_2^{trans}(\vartheta)}{d\Omega},$$

where  $\vartheta, \varphi$  are the polar and azimuthal photon scattering angles, respectively,  $P_e$  is the electron polarization, and  $Q, V$  are the ‘‘Stokes Parameters’’ describing the incident photon polarization ( $Q$  being the linear,  $V$  the circular component). The second term is a nuisance contribution usually eliminated by the use of purely circular light (*i.e.*  $Q = 0$ ). The third and fourth term are those allowing the measurement of the electron polarization; however, since the cross-section is strongly peaked around the beam direction (see fig. 1), the last term vanishes as the  $\cos \varphi$ -dependence is averaged out by photon detectors of commonly used sizes. Thus, switching the photon polarization between right- and left-circular ( $V = \pm P_\gamma$ , where  $P_\gamma > 0$ ) gives rise to a cross-section asymmetry

$$(3) \quad A_{Compton}^{long} = -P_\gamma P_e^{long} \left( \frac{d\sigma_2^{long}}{d\Omega} \right) / \left( \frac{d\sigma_0}{d\Omega} \right) =: P_\gamma P_e^{long} \mathcal{A}^{long},$$

from which the longitudinal electron polarization can be extracted if  $P_\gamma$  is known. Determination of  $P_e^{trans}$  is possible if a position-sensitive detector is used (see *e.g.* [6]).

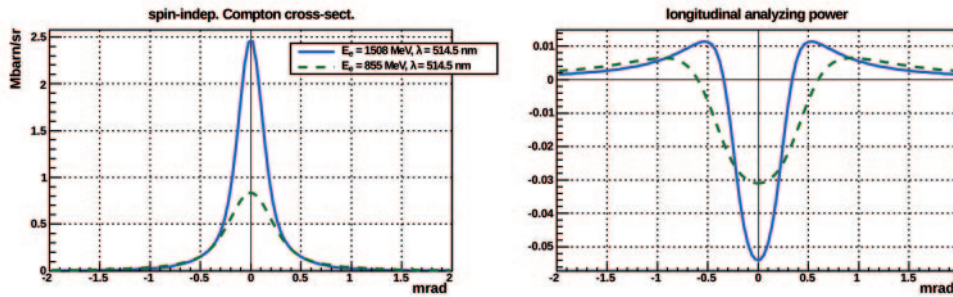


Fig. 1. – Unpolarized cross-section (left) and longitudinal analyzing power  $\mathcal{A}^{long}$  (right), as a function of the lab frame scattering angle  $\vartheta_{lab}$ , for typical operating conditions of the A4 polarimeter (see table IV). Here,  $\vartheta_{lab} = 0$  is chosen to be the beam direction.

**2.2. General layout.** – Compton polarimeters are installed in magnetic chicanes in order to separate the outgoing electrons from the backscattered photons. This design is chosen because it (largely) eliminates any spin rotation between the polarimetry and the PV experiment. The photon source is implemented by a laser in order to provide an intense, focused beam with a highly pure polarization. For the detection of the backscattered photon, which is boosted to gamma-ray energies in the experiments considered here, standard particle detector materials and techniques can be employed. In addition, modern Compton polarimeters use position-sensitive devices to detect the final-state electron. Finally, a polarization measurement device for the laser beam is required in order to determine the “target polarization”  $P_\gamma$  and ensure the correct polarization state.

### 3. – Design concepts and comparison

Different implementation approaches have been chosen for the individual polarimeter components by the various groups operating such devices. The most notable difference is the choice of the laser system, which plays a central role in making Compton polarimetry feasible at the experiments considered here.

**3.1. Laser system.** – The main advantage of Compton polarimetry —non-destructive measurement— turns into a serious challenge at today’s PV experiments which operate at beam currents of significantly less than 1 mA. The resulting low luminosity when using commercial lasers with common c.w. output powers of 10–20 W leads to excessively long measurement times required to achieve reasonable statistical accuracies ( $\mathcal{O}(10\text{ h})$  for  $\Delta P/P = 1\%$ ). Therefore, the laser intensity must be increased.

One solution —the *external cavity approach*— is to feed the output of a commercial laser into a Fabry P erot cavity, wherein constructive interference between incident and recirculating light leads to a resonant build-up of intensity. However, since the achieved gain depends strongly on the fulfillment of the resonance condition ( $l = n\lambda/2$ ), a sophisticated feedback system is needed to ensure the match of cavity length and laser wavelength. Still, such systems have been successfully set up at TJNAF (“JLab”): Hall A uses a high-gain cavity with very high grade mirrors and a demanding stabilization scheme. The original setup, using an IR laser, reached a gain of 7500 and an intra-cavity intensity of 1.7 kW [7]; for the recently performed upgrade to a green laser, preliminary analyses show a gain around 5000 with a power of 5 kW. Hall C uses the same layout, but employs a stronger laser system which relaxes the demands to the cavity gain and thus the feedback system and optics. Preliminary analyses indicate a gain of 100, resulting in an intensity of 1 kW [8]. Although performing well, both setups have the drawback of an explicit crossing angle of 20 mrad between the beams, which reduces the luminosity by about a factor of 20 as compared to the collinear geometry.

A different approach —the *internal cavity approach*— uses the lasing cavity itself: the usable output power of a laser is only a small fraction of the power recirculating inside this cavity; therefore, improvement of the luminosity is possible by extending the cavity, replacing the partial-reflective output coupling mirror with a high-reflective mirror and using the internal power for Compton scattering. Since the laser medium is now inside the cavity, the emission wavelength will adapt to small fluctuations of the cavity length, making an active feedback system unnecessary. Such a system, based on a 10 W Ar-ion laser, has been successfully set up at the A4 experiment at MAMI and reaches intra-cavity powers of up to 120 W. While this is significantly less than is achievable with the external cavity approach, the resulting luminosity is still of the same order of magnitude because a collinear beam geometry was chosen here.

TABLE II. – *Properties of the photon calorimeters used by the Compton polarimeters detailed here. The detectors of the Hall C and A4 polarimeter are segmented ( $2 \times 2$  and  $3 \times 3$ ).*

	JLab Hall A [9]	JLab Hall C [10]	A4 @ MAMI
material	GSO(Ce)	PbWO <sub>4</sub>	LYSO(Ce)
radiation length (cm)	1.38	0.89	1.22
pulse decay time (ns)	30–60	10/30	41
light yield (% of NaI(Tl))	20	0.3/0.08	75

**3.2. Photon detector.** – In most polarimeters, a fast calorimeter (see table II) is used to detect the photons, allowing a measurement of energy spectra rather than just the number of backscattered photons. In this case, several methods to determine the Compton asymmetry are available: in the *counting* (or *integral*) method, only the numbers of backscattered photons for both helicities are recorded. Since the analyzing power changes sign at about half the maximum photon energy (cf. fig. 1), this implies a dilution of the measured asymmetry by the low-energy photons, thus requiring longer measurement times for a given statistical accuracy. This can be alleviated by applying a weighting function: *energy weighting*, for example, emphasizes the high-energy photons which exhibit a large asymmetry, thereby reducing the influence of the low-energy photons (see *e.g.* [9]). The problem is completely eliminated in the *differential* method, in which energy histograms are recorded to extract bin-wise asymmetries. Note, however, that by suitable choice of the lower detection threshold, all methods can be made to perform equally well from the statistics point of view [11]; the main difference is their susceptibility to systematic effects.

**3.3. Electron detector.** – The use of position-sensitive detectors which exploit the dispersion in the rear half of the chicane to measure the energy of the scattered electrons has proven to be essential to the operation of Compton polarimeters (see table III for an overview). In the simplest case, they are used to suppress uncorrelated background, *e.g.* radiation generated by the beam halo [12]. However, they can also serve as a photon tagging device: imposing a coincidence with only one electron detector position channel provides a virtually monoenergetic photon beam that may be used for calibration, in particular for intercalibration of segmented calorimeters at energies beyond the reach of radioactive sources [12]. Tagging can further be used to get hold of systematic effects: for the Hall A polarimeter, dedicated runs recording one coincident histogram for every position channel were taken to parametrize the photon detector response, which was then used to extract the Compton asymmetry from the full spectra taken during regular measurement [7]. In the A4 polarimeter, these tagged spectra are used even for the

TABLE III. – *Types of electron detectors used in recent Compton polarimeters.*

	JLab Hall A	JLab Hall C [8]	A4 @ MAMI
type	Si microstrip	diamond microstrip	SciFi array
layers/channels	$4 \times 192$	$4 \times 96$	$2 \times 24$
pitch	$240 \mu\text{m}$	$200 \mu\text{m}$	$600 \mu\text{m}$

TABLE IV. – Design comparison of the polarimeters presented here. The upper part shows the design potential, the middle part the impact of the experimental conditions (HAPPEx, HAPPEx-III,  $Q_{\text{weak}}$ , and A4), and the lower part the actual performance [7-9,12]. Some simplifications were used in calculating the FOM. All but the Hall A IR performance data are preliminary. Note that the A4 polarimeter has been operated at energies as low as 315 MeV.

	Hall A IR	— green	FOM	Hall C	FOM	A4	FOM
$\lambda$ (nm)	1064	532	$\times 4$	532	$\times 4$	514.5	$\times 4.3$
$P_L$ (W)	1700	5000	$\times 2.9$	1000	$\times 0.6$	100	$\times 0.06$
angle (mrad)	20	20	$\times 1$	20	$\times 1$	0	$\times 20$
$E_e$ (GeV)	4.6	1	$\times 0.05$	1.17	$\times 0.06$	0.86	$\times 0.03$
$I_e$ ( $\mu\text{A}$ )	40	50	$\times 1.25$	180	$\times 4.5$	20	$\times 0.5$
statist. err.	0.6% in 1 h	1.0% in 1 h		1.0% in 1 h		2% in 11 h	
syst. err.	1.4%	0.9%		(0.55 + x)%		(0.45 + x)%	

regular analysis so as to assess the detector response and effects of chicane dispersion and beam position [12]. The Hall C polarimeter, on the other hand, uses the electron detector to get a completely independent access to the Compton asymmetry [8], thereby eliminating many systematic error sources.

**3.4. Laser polarization measurement.** – The standard method to measure the laser polarization is to direct the light onto a rotating quarter waveplate and a linear polarizer, and measure the transmitted intensity, which is modulated at multiples of the waveplate rotation frequency. The polarization state can be extracted from the modulation amplitudes. This method is well-established and accurate, but since the measurement is performed outside the cavity, a systematic change of the polarization has to be expected. In the A4 polarimeter, where one vacuum window placed at  $45^\circ$  serves as a beamsplitter to extract intra-cavity light for polarimetry, the polarization transport matrix of the used window is measured prior to every beamtime in order to take this effect into account.

**3.5. Performance comparison.** – Although quite different in their designs, all polarimeters mentioned in this article have comparable performance potential. This can be seen from table IV, which, taking the Hall A IR design as reference, shows the influence of the design choices and experimental conditions onto the statistical figure of merit [11] —a quantity inversely proportional to the required measuring time.

#### 4. – Conclusions and outlook

Compton backscattering polarimetry is a well-proven method for electron polarimetry, and so far the only non-invasive method available. Techniques have been developed to overcome the challenges at low beam current, and to reach the accuracy of  $< 1\%$  required for the upcoming generation of PV experiments, notably the “green upgrade” of the JLab Hall A polarimeter and the new Hall C polarimeter. Therefore, Compton polarimetry is likely to keep its decisive role in this field of physics research for the near future.

\* \* \*

The author wants to thank W. DECONINCK, M. FRIEND, S. NANDA, A. NARAYAN and K. PASCHKE for useful information on the JLab polarimeters. This article details some work performed by the author together with other members of the A4 collaboration which is supported by the German DFG. It comprises parts of the author's Ph.D. thesis.

#### REFERENCES

- [1] BAUNACK S. *et al.*, *Phys. Rev. Lett.*, **102** (2009) 151803.
- [2] PASCHKE K., talk presented at this conference.
- [3] ANDROIĆ D. *et al.*, *Phys. Rev. Lett.*, **104** (2010) 012001.
- [4] CHUDAKOV E. and LUPPOV V., *IEEE Trans. Nucl. Sci.*, **51** (2004) 1533.
- [5] LIPPS F. W. and TOLHOEK H. A., *Physica*, **20** (1954) 395.
- [6] DOLL D. *et al.*, *Nucl. Instrum. Methods A*, **492** (2002) 356.
- [7] ESCOFFIER S. *et al.*, *Nucl. Instrum. Methods A*, **551** (2005) 563.
- [8] NARAYAN A., these proceedings.
- [9] FRIEND M., these proceedings.
- [10] DECONINCK W., private communication.
- [11] BARDIN G. *et al.*, Technical Report DAPNIA/SPhN/96-14, CEA, 1996.
- [12] DIEFENBACH J., PhD thesis, Johannes Gutenberg-Universität Mainz, July 2010.